Russell Christopher, T. (Orcid ID: 0000-0003-1639-8298)
Jian Lan, K (Orcid ID: 0000-0002-6849-5527)
Luhmann Janet, G (Orcid ID: 0000-0003-0626-9353)

The Solar Clock

C. T. Russell[1], L.K. Jian[2], and J. G. Luhmann[3]

[1] Earth Planetary and Space Sciences, University of California, Los Angeles.

[2] Goddard Space Flight Center, National Aeronautics and Space Administration, Greenbelt, MD.

[3] Space Sciences Laboratory, University of California, Berkeley.

Corresponding author: Christopher T. Russell (ctrussell@igpp.ucla.edu)

Key Points:

- The nuclear furnace inside the Sun is steady but the visible surface of the Sun changes quasiperiodically with an 11-year average cycle.
- The quasiperiodicity begins at the tachocline when the heat flow changes from radiation to convection.
- The phasing of the sunspot cycle varies over time scales of decades but is an accurate clock on the time scales of centuries.

This article has been accepted for publication and undergone full peer review but has not been through the copyediting, typesetting, pagination and proofreading process which may lead to differences between this version and the Version of Record. Please cite this article as doi: 10.1029/2019RG000645

Abstract

The Sun is powered by a very stable source of fusion energy in its core that radiates that energy outward in a constant flow. Yet it has a cycle of magnetic dynamo activity whose strength and duration are variable. This variability, which affects the Earth's 'space climate', points to temporal changes in the convective and diffusive transport of magnetic flux above the tachocline, where the flux is generated. The longest record we have of this variability is the time series of Sunspot Numbers (SSN). This record suggests that the interior of the Sun follows a clock-like magnetic flux production cycle with a length of close to 11.05 yr. The variations in sunspot cycle duration, as well as the sunspot number rise and fall times, their hemispheric asymmetries, and the maximum sunspot numbers of the individual cycles, are likely produced in the process of the magnetic flux transport. Helioseismology continues to shed more light on the convection zone variabilities, including the 'torsional oscillations' that seem to have a special connection to the emerging strong magnetic fluxes that produce the sunspots. These new observations may eventually lead to an explanation for the surprisingly good correlation between the rate of sunspot appearance and the maximum sunspot number, and to a better understanding of the relationship between the solar dynamo and the sunspot number cycle. Better understanding of the polar regions awaits long-term monitoring with a polar solar mission. Better predictions of near-term space weather could be obtained from a permanent L5 monitor.

Plain Language Summary

The Sun is a giant rotating ball of electrically conducting material that has existed for approximately 4.5 billion years, burning hydrogen, turning it into helium, and producing energy that radiates upward toward the Sun's surface. This process is steady deep inside the Sun, but the surface of the Sun is far from steady. At about 70% of its radius, the transfer of the nuclear heat becomes more efficient if it is transferred by convection and overturning rather than radiation. The rising, spinning, electrically conducting liquid in the outer solar layer produces a magnetic field that reverses every sunspot number cycle. These cycles vary in length from about 9 to 13.6 years, but average close to 11 years. The sunspot numbers in the southern and northern hemispheres are somewhat independent and peak at different times with different amplitudes. The variations are consistent with the diffusion of magnetic fields in a non-ideal conductor. The sunspot numbers appear to have long-term cyclic behavior. The durations of these grand cycles are difficult to predict. The Sun seems to be a dependable power source, but predicting the strength and timing of its cycles is difficult.

1 Introduction

In this post-industrial age of global communication and super computers, we are increasingly sensitive to the effects of solar activity on our technological systems, including its associated influxes of energetic particles, ionospheric disturbances and geomagnetically induced currents [*Russell et al*., 2015]. When the solar cycle is very active, our space-based systems, including advanced communication satellites and navigation networks, are increasingly affected. Thus, it is important both to know the possible range of future solar activity, and to anticipate when significant changes will occur. One approach is to seek clues in the historical observations of sunspot numbers. Although there are many other solar surface (and now interior) features that have been tracked for more than a cycle [e.g. *McIntosh et al*., 2014], the sunspot numbers have a much longer record than other solar activity-related observations [e.g. *Kitiashvili and Kosovichev*, 2008]. In addition, because we can now better relate sunspot number to these other features, it may be possible to draw new meaning from this simple time series. This paper examines some of these connections, e.g. of the sunspot cycle, to recent helioseismology results and models of the observed magnetic field on the solar surface. By looking deeply into the past, which the use of sunspot numbers uniquely allows us to do, we may better extrapolate into the future.

That the number of sunspots seen on the solar disk undergoes nearly periodic cycles of from 9 to 13.6 years duration (see Figure 1) was noted long ago and documented by the earliest solar astronomers. This variable behavior reveals the dichotomy between the steady input from the Sun's nuclear furnace and the release of that energy into the heliosphere.

Sunspots occur in latitudinal bands that migrate equatorward through the solar cycle from starting latitudes around 30°. This migration gives rise to the 'butterfly diagrams' shown here. A complementary diagram is the sunspot area diagram (Figure 1, bottom). Clearly some cycles had significantly more sunspots than others both in number and in area. Over time, much work has been devoted to accumulating and analyzing the time series of sunspot numbers, with goals ranging from basic phenomenology to physical interpretation [e.g., see *Svalgaard*, 2013; *Hathaway*, 2015].

We now appreciate that the sunspot cycle includes a magnetic polarity flip every sunspot number cycle so that the solar magnetic cycle is about 22 years long. However, as the title of this review suggests, we wish to stress the very important but often overlooked aspect of solar activity, that it is controlled by a quite constant clock. To address this point, we need to have as long a time series as possible. Thus we will start with solar cycle 1 in 1750, and continue to solar cycle 24. While it takes the Sun 22.1 years on average to go through a solar magnetic cycle, there is no reason to believe that the physics of sunspots changes between the cycles with different polarities. We obtain this average sunspot period of 11.05 yr by simply dividing the time since the first sunspot minimum and the most recent one by the number of sunspot cycles in between. If the Sun is an accurate clock, this period becomes more accurate the longer a time series is available.

This figure also serves to introduce a few caveats concerning the use of sunspot number alone. One can see that the 'butterfly wings' in the upper panel of Figure 1 sometimes overlap for adjacent cycles, and they may also appear quite different in density and/or shape in the northern and southern hemispheres.While this does not render the long sunspot record useless, it does make the definition of the solar minimum less reliable in terms of an absolute state of minimum solar activity than the sunspot maximum is for establishing the maximum of activity for a cycle. At the same time, differences in timing of the maximum of the sunspot number in the northern and southern hemispheres make the definition of a single sunspot cycle maximum less definite [e.g., *Temmer et al*., 2006; *McIntosh et al*., 2013]. These caveats need to be kept in mind when patterns of its behavior are investigated or assumed. Another caveat is the fact that the solar cycle is actually a ~22 year cycle when its magnetic state is taken into account. This underlying fact cannot and should not be ignored in analyzing sunspot numbers, although magnetic field information is missing for the longer record. On the other hand, since there is no reason to expect that the physical processes depend on the polarity of the Sun's overall magnetic field, we can treat the sunspot cycles as independent cycles. We start with cycle 1 starting in 1755, and continue to present solar cycle 24 in this review.

Most agree that the origin of sunspots is tied to the solar magnetic cycle [e.g. *Rempel et al*., 2009]. As illustrated in Figure 2, inside the Sun, a nuclear fusion furnace generates energy that is radiated upwards quite uniformly and steadily until it reaches the tachocline at a radial distance at ~0.7 Rs, where convective heat transport becomes more efficient than radiative transport. The convection and rotation in the convection zone at and above the tachocline act together to produce concentrations of strong magnetic fields that through a combination of buoyancy and diffusion make their way to the surface. A sunspot forms on the solar photosphere where the magnetic field is sufficiently strong to develop an organized structure that cools the surface in the neighborhood of the enhanced field. The cooling causes a drop in luminosity, i.e., the sunspot. The generation of the flux that makes sunspots thus occurs deep in the solar interior.

Several huge leaps in understanding the solar cycle came with the advent of the magnetograph [*Hale*, 1908] and helioseismology [e.g. *Thompson*, 2004]. The ability to observe the magnetic polarity patterns of not only the sunspots but the background solar surface established the existence of the solar magnetic cycle of ~22 years. These observations further showed the relationships between the solar polar magnetic fields and the fields of active regions and the sunspots within them. For example, phase shifts exist between the magnetic (Hale) cycles of the large-scale fields at the poles and the polarity patterns of the bipolar active regions (with and without spots). There are systematic tilts of the magnetic axes of the bipolar active regions in each hemisphere, such that the leading (in the sense of solar rotation) polarity tends to match the large scale polar magnetic field in the same hemisphere. That the leading polarity tends to be closer to the equator was established early in the magnetograph era. It is still a holy grail of solar cycle theorists and modelers today. These observations, illustrated by the center full-disk magnetogram in Figure 3, also reinforces the idea that there are overlaps between solar cycles, as the polar field reversals occur around solar maximum which is somewhere in the middle of the polarity cycle of the active regions. The magnetic polarity of sunspots generally follows the active region polarity cycle. However, around solar minimum there is a transitional mixture of old cycle and new cycle spots, and ephemeral active regions of a new cycle can appear as early as in the declining phase of a previous cycle [*Wilson et al*., 1988]. There is unfortunately no magnetic field information for the long term sunspot number record before cycle 18, thereby restricting one to investigate the numbers alone. Still, the knowledge of the cycling of the sunspot magnetic field polarities, and their relationship to the active region fields, is useful to keep in mind.

The convective dynamics of the outer layer of the Sun enables the use of seismological techniques to look inside the Sun. Inversion of the 5-minute oscillations seen at the solar surface has allowed us to determine the radial structure and circulation of this thick outer layer as shown in Figure 4 (left panel). At the depth of the tachocline, at the bottom of the convection zone, important changes occur in the interior dynamics of the Sun over a relatively narrow layer. This essential result from helioseismology revealed that while the interior radiative zone rotates rather rigidly at the Sun's average ~27 day rotation period, the overlying convection zone rotates differentially, with the equatorial region moving faster and the polar region moving slower than the radiative zone rate. This produces velocity shears of different signs at the tachocline whose consequences are considered the roots of the solar cycle [e.g. *Charbonneau*, 2010; *Cameron et al.*, 2016, and references therein]. In addition, as illustrated in Figure 5, there are two other patterns of large-scale convection that are of interest: One consists of meridional (longitudinal) cellular motions that tend to be poleward near the surface and have return/equatorward flows at depth, and the other consists of torsional oscillations –alternating bands of zonal (latitudinal) flows that are superposed on the average differential rotation pattern and migrate equatorward with the sunspot belts as the solar activity cycle progresses. It is believed that strong toroidal magnetic flux generated near the tachocline is transported toward the surface where a small fraction of it emerges in the form of bipolar active regions that include sunspots. Sunspots are thus a product of the combined internal flux generation and transport processes, a concept that will arise again in the discussion below. In general, the area covered by sunspots and the sunspot numbers have been excellent proxies for the intensity of solar activity in all its forms, including solar irradiance variations, solar flares, and coronal mass ejections.

When a long deep sunspot minimum occurred at the end of cycle 23, we wrote a review revisiting solar activity trends [*Russell et al.*, 2010] motivated by expectations of a significant change in the sunspot behavior in cycle 24. The downward trend in solar activity, first widely appreciated during cycle 23, indeed continued through the cycle 24 maximum. As we approach the end of cycle 24, having descended into another deep minimum, we are again motivated to assess whether there are predictive clues in the time history of sunspot numbers. Much recent work has involved analyses of the solar polar field strength available for a limited number of cycles [e.g., see *Pesnell and Schatten*, 2018], but here we choose to focus on the longer perspective provided by the sunspot number record. Although sunspot number trends have been analyzed for decades, each new cycle, especially when combined with new insights into the operation of the solar dynamo, potentially contributes to its interpretation. Figure 6 shows the updated sunspot number (SSN) record recently compiled and archived as the Sunspot Index and Long-term Solar Observations (SILSO) at the Royal Observatory of Belgium [*Clette and Lefèvre*, 2016]. The average length of solar cycles 1-23 is 11.05, with a standard deviation of 1.17. The average number of maximum SSN is 178.7. Thus, we add a dotted line in Figure 6 to represent a rectified sine wave in which the minima are 11.05 yr apart and the SSN maxima are 178.7. This is the best, least-square rectified, sine-wave fit to the sunspot cycle from 1750 to 2018. Low SSN counts occurred in cycles 5, 6, 7, 12-14, 16 and in cycle 24 from 1750-2018. A large phase shift built up before cycles 5 and 24 gauged by our 11.05 yr clock. Less phase shift built up before the slightly weaker cycles 12-16. This behavior is suggestive that there is an overall fixed period for the dynamo, but the transport process between the dynamo and the surface can be faster or slower and advance or delay the maxima, with consequences for their strength because the magnetized fluid is diffusive. Early empirical relationships showing correlations between the cycle maximum and rise time or rate [*Waldmeier*, 1935] provided one of the most important clues toward a deeper understanding of this behavior. In the paragraphs below we discuss the current state of knowledge of the Sun as it relates to the interpretation of the sunspot cycle, to both encourage those analyzing the latter to incorporate deeper implications in the design of their studies, and to point out some outstanding areas of related research still in need of further developments. We will return to this time series in Section 4 after discussion of the solar dynamo.

2 Early Thoughts on the Solar Dynamo

The solar magnetic field must be generated by a magnetic dynamo inside the Sun. If so, how might it work? And how are the surface observations related to its operation? In the 1960s, the use of the 5-minute oscillations to peer inside the Sun had not even been hypothesized, let alone utilized. The early framework for explaining the sunspot cycle was the Babcock-Leighton dynamo [*Babcock,* 1961; *Leighton*, 1969], which internally generated a toroidal field from a poloidal field to start the next cycle. In this model, the differential solar rotation inferred from observations played a key role by winding up the longitudinal (poloidal) magnetic field threading the solar interior. When the resulting toroidal field became strong enough, it was envisioned to erupt through the surface in bipolar patches of strong field, the active regions. The model also assumed that the emerging flux had a bipolar field with axes tilted with respect to the solar equator and emerged kinked in such a way that the poloidal fields of emerging active regions eventually reversed the global poloidal field. These ideas were later incorporated into surface flux transport models [*Sheeley*, 2005; *Hathaway and Upton*, 2016; *Wang*, 2017] that numerically model the convective and diffusive transport of the magnetic flux that emerges onto the solar surface with the patterns prescribed by the observed sunspots. The models, which can reproduce the long-term patterns of solar magnetic cycles seen on the surface [e.g. Wang et al., 2005], can obtain opposing flux concentrations at the poles that have about the right magnitude, timing and phases to match the observed polar field reversals. But the processes occurring below the surface of the Sun that set the stage for the cyclic behavior on the surface are neither explicitly included, nor revealed. The reason why surface flux transport models appear to work so well in spite of this remains an outstanding problem in the physics of the solar cycle.

3 Peering Beneath the Surface

As shown above in Figures 2 and 4, our modern understanding of the Sun, informed by helioseismology [e.g. see *Miesch*, 2005, and references therein], contains a radiative core that effectively heats the overlying layers from the bottom. At about 0.7 Rs, heat transport becomes more efficient if the material there convects rather than radiates. A pot of water slowly heated on a stove provides a simple analogy. The water convects upward and transports the heat applied to the bottom of the pot to the surface of the water. However, the situation on the Sun is much more complex than on the stove because the solar pot is spinning and the fluid is magnetic. Transport of angular momentum in a convecting rotating spherical shell is complicated. A rotating cylinder of uniform density can develop rotating columns of fluid first described by Kelvin [*Fuentes*, 2009] and later by *Taylor* [1922], called Taylor, or Taylor-Proudman, columns. In a convecting spherical shell of finite thickness the motion of the fluid is even more complex. Moreover, the material in the Sun has finite electrical conductivity and a magnetic field that can exert significant force on the convecting fluid, leading to the observed rotational behavior in Figure 4. In a case with a strong and dominant internal dipole field, the convection zone might be forced to corotate, As *Howe et al*. [2009] show, the solar case is somewhere in between the Taylor-Proudman column state and differential rotation that depends only on latitude. Their figure, reproduced below as Figure 7, suggests what successful models of the solar convection need to aspire to. They also suggest that this pattern may dictate the location where the shear velocity at the interface with the tachocline expedites the strong flux emergence from below.

The surface flux transport model cannot adequately incorporate the behavior of this clearly three-dimensional, turbulent, electrically-conducting, and magnetically-coupled system. *Dikpati et al.* [2006] and *Dikpati and Gilman* [2006] constructed an internal flux transport dynamo model with Hadley-cell-like convection carrying magnetic flux poleward near the surface, downward at the poles, and equatorward along the bottom of the convection zone. This model could explain some of the trends seen in solar cycles as observed in the large-scale surface field. Choudhuri and coworkers [e.g. *Chatterjee et al*., 2004; *Choudhuri*, 2006, 2008] developed competing models where diffusive magnetic flux transport played an important role in the interior flux circulation. Since that time, a number of global numerical dynamo models have been developed [e.g. *Charbonneau*, 2010; *Cameron et al*., 2016] that include more of the applicable physics. Most importantly, helioseismology has improved because of better observations and new analytical and observational techniques, allowing the diagnosis of the large-scale circulation patterns within the entire convection zone covering most of cycles 23 and 24 [*Komm et al.*, 2018].

Moreover, these models bring new appreciation of the torsional oscillations and their bearing on the surface magnetic field. They were first characterized in the surface zonal flows by *Howard and Labonte* [1980], and have now been characterized in the subsurface data by *Howe et al.* [2000, 2009]. These departures from the average differential rotation pattern appear each cycle near a latitude of 50-60 degrees close to the time the polar field reverses at solar maximum and migrate equatorward. When they reach about 30 degrees, the active regions of the cycle begin to emerge and move equatorward along with the torsional oscillation. At the same time, a poleward branch of the torsional oscillation is born that persists until the active belt reaches the equator. Recent reconstructions of both the zonal and meridional flows inside the Sun [*Komm et al.*, 2018; *Kosovichev and Pipin*, 2019] show that these deviations from the average flow patterns exist throughout the convection zone, and evolve with the activity cycle. Figure 8 shows some of these data from the latter authors, with the average rotational velocity subtracted from the measured zonal (latitudinal) velocity in the bottom panel (b), and corresponding longitudinally averaged surface magnetic field (panel a) for comparison. Questions these observations have raised include why the flow deviations precede the appearance of the magnetic flux emergence on the surface (active regions and their sunspots), and why the magnetic features' average locations correspond to locations of high velocity shear [*Kosovichev and Pipin*, 2019]. The diagrams clearly show that the solar cycle consists of nested 22-year cycles and that solar minimum does not mark a period of stoppage of the solar cycle, rather the system has memory across the solar minima.

The additional appearance of local control of surface velocities by the presence of active regions, in the form of convergence toward them, reinforces belief in the importance of feedback from the magnetized plasma on the flows via either Lorentz or thermal forces [*Kosovichev and Zhao*, 2016]. Some solar cycle modeling experiments have tried to incorporate such effects, including simulations of the torsional oscillation patterns that would result from different forcing functions [*Rempel*, 2007], and to consistently reproduce Waldmeier-like relationships in their surface magnetic fields [e.g. *Pipin and Kosovichev*, 2011]. Both these and the surface flux transport models require additions to their physics in the form of still ill-defined processes needed to transform a fraction of the tachocline-generated toroidal magnetic flux to poloidal flux, and a more accurate description of diffusive transport that includes field dissipation. Additionally, meridional circulation, typically characterized as poleward flows in each hemisphere, may indeed reverse to equatorward flow at high latitudes during the active cycle phases, as also inferred from some surface flux transport models [e.g. *Cameron et al.*, 2014]. Hemispheric differences in both the zonal and meridional flows that relate to sunspot number and distribution also exist [e.g. *Kosovichev and Zhao*, 2016].

There are thus many essential features and processes in the convection zone that can contribute to solar cycle variations: the extraction of magnetic flux from the major shear zone at the tachocline; the behavior of the convection zone flows on all scales; and the process of magnetic flux transport and circulation, including relatively undefined dissipative, active region formation, and emergence processes. Referring back to the SSN time series discussion, it is easy to see how magnetic flux produced on a relatively regular 11.05 year underlying 'clock' cycle can give rise to SSN cycles with variable strengths, phasing, and hemispheric differences. Although Waldmeier found a strong relationship between the cycle rise rate and maximum sunspot number that seems to hold promise for constraining these, *Karak and Choudhuri* [2011] found that a variety of models and assumptions could reproduce that result –leaving the search for consistent behavior between solar surface and interior cycles still open [see *Karak and Miesch*, 2017 for example].

The Earth has a dynamo in its deep interior with a solid core beneath it [*Lehmann*, 1936]. This solid core and the order in the liquid core flow imposed by rotation minimize the communication between the north and south polar regions of the Earth's magnetic dynamo. As a result the magnetic fields over the two poles can act independently [e.g., *Schaeffer et al.*, 2017]. The Sun too has a central non-convecting region that includes a much larger fractional volume than the Earth's solid inner core (see Figure 2). Thus we would expect independent hemispheric behavior over a much larger portion of the Sun's polar regions than the Earth's polar regions. In other words, there should not necessarily be north-south agreement in either the times when solar activity maximizes, the number of sunspots at the maximum, or the polar magnetic fields of the Sun. Moreover, hemispheric differences should be present in the entire convection zone below. We note that the north-south asymmetry in solar activity has in some cases been interpreted in terms of a coexisting quadrupolar dynamo-driven moment [e.g. *Schussler and Cameron*, 2018]. The independence of the polar circulations is a likely mechanism for producing the quadrupolar moment, in close analogy with the situation inside the Earth [*Cao et al*., 2018]. Thus, the observation that the timing, as well as the magnitude of the sunspot maximum can be different in the two hemispheres should not be surprising. However, how the hemispheres interact with one another must also influence the cycle strengths and progressions.

There has been much qualitative discussion, and some modeling, of how variations in convection vs. diffusive transport and decay (which can also be thought of as resulting from turbulent convection) determine the fate of magnetic flux generated in the tachocline shear zone [e.g. *Chatterjee et al*., 2004; *Passos et al*., 2013]. If the amount of flux generated at the tachocline were the same each solar cycle, its strength at the surface should be lower at solar maximum for more slowly rising cycles because there would be more time for dissipative processes to act in the convection zone as the generated flux rises. This would be consistent with the Waldmeier effect, which could be explained if faster transport through the convection zone minimizes this diffusive decay. Also, when stronger magnetic-field survives the trip, more sunspots should form.

Dicke [1978] appears to be the first strong proponent that deep in the Sun, the solar dynamo is paced by an accurate internal clock, and the observed sunspot number cycles have durations that fluctuate about that period, but in the long run, the period averages to a constant number. The sunspot number cycle sometimes appears to advance steadily, but eventually it snaps back to the phase that would have accrued with a regular period (close to 11.05 yr) after several cycles. When we wrote our review of the sunspot cycle near the end of cycle 23, it was not clear that such a snap back would occur, but if it did, that historically one might expect the following two or three cycles to have weak activity. Indeed, cycle 24 has proven to have a weak sunspot maximum. Such periods have been used to define a 'Grand Cycle' that forms an envelope of the sunspot maxima [cf. *Pipin and Kosovichev*, 2018].

4 A Dynamo Master Clock?

This controlling ‘clock’ is illustrated above in Figure 6, where a dotted reference cycle with an amplitude of 178.7 (the average of the maximum sunspot numbers obtained from all 24 cycles shown) and a period of 11.05 years (the average of the sunspot cycle periods for cycles 1-23) is superposed on the updated sunspot number time series. The phase of this curve was chosen so that the maximum of cycle 1 was aligned with the observed sunspot maximum. The first ‘snapback’ of phase, the notion introduced above, occurred at the end of cycle 4 where our chosen period centers cycles 5, 6 and 7 to match the ‘clock’ phase existing in cycle 1. The vertical solid line marks the end of the first ‘Grand Cycle’ defined as the interval over which the solar cycle phase changes ending in a snapback, and the start of Grand Cycle two. A much weaker phase deficit builds up in cycles 8-11 and disappears during the next three “weak” cycles 12-14. More important is the fact that the 11.05-year period keeps these cycles aligned with the prevailing, underlying clock in the longer term. Cycle 15 is chosen as the first cycle of the new Grand Cycle because the maximum sunspot number reaches the value of the long-term average sunspot number. The next solid vertical line between cycles 14 and 15 begins a period of generally increasing solar maxima, through cycle 19 with its much stronger than average maximum, until cycle 23, at which time a substantial phase deficit has again accrued. Cycle 24 is now known to be weak and its phase is more aligned with our clock phase. This periodic realignment of phases was a key element in Dicke’s [1978] advocacy of a solar clock. For plotting purposes, we have assumed cycle 24 ends in mid-2020. Whether this is a perfect match requires cycles 25 and following to assess. If the durations of past intervals of phase lags are a guide, the current phase lags may persist at least several more cycles, to be followed by a period of notably weak solar maxima. Regardless of whether a phase deficit precursor to weaker cycles is a reality, its apparent occasional appearance may indicate that it is part of a ‘Grand Cycle’ of solar variability, an interpretation whose usefulness will depend on having a longer sunspot record to establish its rules of application.

While Figure 6 shows well the behavior of the peak solar activity, it does not show well the shape of the activity curve. In Figure 9, we show each sunspot cycle on a scale sufficient to resolve its temporal behavior, including the occurrence of multiple maxima, as indicated by vertical dashed lines. It is worth noting here that there is an implicit relationship between the apparent variations in phase of the sunspot cycle, and the rise and decline times and rates of sunspot numbers. For example, the numbers of spots and the strong spot-producing fields of a strong cycle may take longer to decay, interfering with the growth of the new cycle, with the result that the subsequent cycle is both delayed (phase shifted) and has a shorter time to grow-relative to the flux production clock. If there are more than one time points of minimum SSN, the minimum time is set as the median of these time points. If there are two SSN peaks for a solar cycle, we select the mean peak time as the final peak time. The rising phase is from the minimum SSN to the next peak SSN time of a solar cycle, while the declining phase is from the peak SSN time to the next SSN minimum. In Figure 10, we plot the maximum sunspot number of a cycle versus the ratio of the duration of the declining phase (Td) versus the rising phase (Tr). If we examine the shapes in Figure 10, we see that cycle 4 on the far right has the highest Td/Tr ratio. It was followed by cycles 5, 6, 7 that have low sunspot maxima. The second largest ratio of Td/Tr is cycle 11 and its following cycles 12, 13, 14 also have low sunspot maxima. However cycle 23 that preceded low sunspot maximum cycle 24 did not have a high Td/Tr ratio. Figure 9 illustrates a possibly important difference between cycles 4 and 11, and cycle 23. Cycles 4 and 11 were dominated by a single peak while cycle 23 had two nearly equal and well separated peaks in activity. Had one calculated the Td/Tr based on the initial rise time only and not the average of multiple SSN peaks, the result would be more in line with the behavior after cycles 4 and 11. Thus, while the SSN cycle phasing may not provide the ideal indicator of future solar activity, it appears that the sunspot number behavior is reflecting some subsurface controls that keep their average cycles in synchronization with the internal dynamo clock.

A possibly related fact is that sometimes the sunspot number cycles in the northern and southern solar hemispheres appear significantly (by up to several years) out of phase, and/or have significantly different levels of activity at the two poles. This property has been associated with weak solar activity [e.g. *Temmer et al*., 2006]. Svalgaard and Kamide [2013] have noted that the hemisphere with the strongest activity is the one that peaks first. This correlation of strength and rapid appearance makes physical sense in this diffusive medium. Since diffusion weakens fields, faster delivery produces stronger fields.

Figure 11 shows the sunspot number record from 1950 through 2018 where the data from the two hemispheres have been separated. Here, the color green shading highlights the interhemispheric difference when there is an excess in the north, and red, where there is an excess in the south. Notably there are hemispheric asymmetries in all cycles, but the fractional differences appear to be larger (up to a factor of ~2) for many of the weaker cycles shown. The timing of the maximum SSN can be different in the two hemispheres by up to several years, having the complicating effect of producing more than one ‘solar maximum’ for a cycle. For the last cycle shown in this plot, which is also the weakest cycle in this series, both the phase separation of the hemispheric SSN maxima is pronounced, as is the hemispheric maximum number difference. However, like the phase shifts with respect to a fixed ‘clock’ period described above, this impression is not straightforward to quantify. This analysis is also compromised by the lack of the longer duration record of hemispheric sunspot numbers.

What is probably the best finding relevant to cycle activity prediction from the sunspot number time profile centers on the well-known relationship between the rate of rise of the sunspot number time series and the ultimate cycle amplitude established by *Waldmeier* [1935]. Figure 9 showed the full-disk sunspot numbers in the updated record plotted separately for each cycle with vertical lines showing the locations when two principal maxima (some from the hemispheric differences) exist. Note the northern hemisphere was much stronger than the southern one in cycle 19, thus only one peak appears in the total SSN plot in Figure 9. For our reanalysis of the updated SSN time series, we use the central time between these two maxima to determine the time for the rise to maximum activity and the decline to minimum activity. Using the peak sunspot number that follows, the remarkably positive correlation in Figure 12 is seen. This exceptionally clear correlation, used for solar cycle interpretation, modeling, and prediction, is sometimes referred to as the second Waldmeier effect because its originator had also found an inverse relation between cycle rise phase duration and the SSN maximum [e.g. *Karak and Choudhuri*, 2011]. One major caveat is that this analysis requires determination of the rate of SSN rise, which is sensitive to both overlaps in sequential cycle sunspot populations, and uncertainties associated with fluctuations in the apparent slope of the rising phase. In addition, as discussed above, there are also hemispheric differences in the cycle time profiles. Does the Waldmeier analysis applied to the individual hemispheres show the same behavior? In Figure 12 we plot the two hemispheric SSN counterparts and total SSN. While the basic positive trend of rise rate vs maximum SSN is present for both hemispheres, the slopes are somewhat different. Users of the Waldmeier relationship based on full disk SSN for anticipating the cycle maximum should be aware of such influences. Also, applying this relationship to the prediction of the new cycle (cycle 25) requires a sufficient amount of time –perhaps several years- after new cycle spots first appear on the disk to confidently establish SSN rise rate.

The foregoing discussion generally reinforces conclusions reached by others who have studied the long term SSN time series toward understanding activity level trends and making cycle predictions. These empirical results support the notion of a regular deep solar dynamo that produces magnetic flux on a nearly constant cycle ('clock'), while the transport of that flux to the surface and the related formation of sunspots determine the SSN time series. As Dicke [1978] noted, the transport time for magnetic flux from the generation depth is sufficiently long to explain the varying sunspot number cycle phase even given a perfect dynamo clock.

Only recently [*Komm et al*., 2018] has the inversion of the helioseismic data taken into account the north-south asymmetry of the solar convection pattern. Sunspot numbers are affected by these internal asymmetries. As discussed above, the hemispheric SSN record in Figure 11 shows the pattern of north-south asymmetry over cycles 19-24. It also shows there can be a dominant hemisphere for the duration of a full cycle, and that sequences of several cycles can exhibit the same hemispheric bias. It should be mentioned here that although a relationship between hemispheric asymmetry and cycle maximum SSN has not been established, it has been suggested that there is a longer-term periodicity in the preferred hemisphere, possibly associated with the proposed Grand Cycle [e.g. *Murakozy and Ludmany*, 2012; *Schussler and Cameron*, 2018]. (If their pattern persists, cycle 25 will have dominant northward activity.) Perhaps the physics of the hemispheric asymmetries can tell us something about the physics of the sunspot cycle itself.

As illustrated in Figure 2, the radiation zone acts to separate north and south polar convection zones allowing the north and south polar caps to have some magnetic independence. At mid and low latitudes above the tachocline, the solar interior behaves like a fluid in a spherical chamber. These phenomena are altered by geometry and radial variations of density, so simple descriptions of the convective motions in the solar convection zone in those terms are difficult, but the analogy of interest here is at the higher latitudes. The quasi-independence of the two hemispheres is associated with the existence of the large non-convecting core. This introduces independent dipole magnetic moment contributions in the two polar regions, which in turn create a global quadrupole. This adds to the hemispheric asymmetries in some sunspot cycles as well as potential shifts in cycle phasing. While there may be predictive power in the slow rise rate of the solar cycle for predicting weak solar maxima, the quasi-independence of the magnetic fields of the two polar regions may interfere with its reliability.

Earlier we mentioned the torsional oscillations, departures of the zonal flows from the nominal differential rotation pattern that evolve in space and time with the solar activity cycle throughout the convection zone, whose role in the sunspot cycle is continuing to be appreciated. This is one of the internal convection properties showing hemispheric asymmetries that begin at high latitudes, possibly where the subsurface convection zone becomes divided by the presence of the core. The challenge is to find the physical connections between all of these observations that ultimately affect the sunspot cycles.

5 Conclusions

Much has been made of the polar field magnitude at solar cycle minima as a means of anticipating the strength of the following sunspot maximum [e.g. *Schatten et al*., 1978; *Svalgaard*, 2013; *Hathaway and Upton*, 2016 and references therein]. These works make the implicit assumption that the polar fields seed the process of the subsurface flux emergence that leads to sunspots. Notably, there are gaps in understanding how such seeding/recycling might occur. Sunspot number provides a much longer record for establishing trends than does the solar magnetic record. The modern sunspot record as recently updated [*Clette et al*., 2014; *Clette and Lefèbvre*, 2016; *Clette et al*., 2016a, 2016b] has an advantage over other observations available for a shorter period for both establishing the regularity (and period) of the solar 'clock', and toward interpreting what the phases, the rates of rise and fall, and the sizes of the maxima tell us about the solar dynamo and the transport of magnetic flux to and from the surface of the Sun.

We have examined the updated record of the sunspot number time series over the last 260 years to revisit some of the clues in the different cycles as to how the solar dynamo operates. It seems clear that the Sun generates magnetic flux with a regular internal clock that has a period of close to 11.05 years. But the magnetic field of the photosphere as represented by the number of sunspots is quite variable. This variability appears to be due to varying transport rates from the source region together with varying decay rates as the cycle evolves. What controls the transport rate is not clear, although observations and models suggest both convective and diffusive transport vary from cycle to cycle. The different appearances of individual sunspot cycles, including their numbers and time profiles, point to a range of conditions for surface delivery associated with the variable, turbulent convection between the flux-generating layer in the tachocline and the surface.

The north-south asymmetries seen on the Sun may provide some especially important clues to the coupling between the solar dynamo clock and the visible Sun. Typically, dynamo models have assumed the hemispherically symmetric circulation pattern shown in Figure 5. Helioseismology is now telling us this is not accurate [*Komm et al*., 2018]. Its underlying causes and consequences have yet to be explored. We note there is an apparent current minimum number of sunspots at cycle maximum based on the updated sunspot number record. In the modern epoch covered by the sunspot number time series there are always more than about 80 spots per month at solar maximum. The Sun has not recently had a cycle without sunspots, even though the observations during the Maunder minimum suggest this can happen. If we could understand what conditions would make a spotless Sun that then recovers, we would probably be able to explain the more modest variations we see today.

The uniquely long duration sunspot number record is a rich source of information but now it needs to be interpreted in light of the growing knowledge of both magnetic transport from the deep seated dynamo region to the surface, and its evolution. Recently, a number of solar dynamo researchers have recognized the possibly important role of the torsional oscillations in the solar rotation in the modulation of cycle activity ranges, and as another possible precursor/predictor of cycle progression [e.g. *Kosovichev and Pipin*, 2018]. This cyclic part of the internal convection appears to be a result of the flows interacting with the magnetic fields in ways that can be both reactive (flows responding to fields) and transformational (field emergence being affected by the flows) [e.g. *Mahajan et al*., 2018]. The torsional oscillation is a challenge that remains to be addressed as is the influence of the division of the convection zone into separate polar and low latitude cells noted above. It is clear too that like the solar interior, the polar regions need to be monitored more regularly as they are a key to understanding both the flux transport cycles, and the reasons why cycles are often hemispherically asymmetric. Is the appearance of an important quadrupolar contribution of the dynamo a cause or result of a weak or asymmetric cycle?

Since neither pole alone may be representative of the state of the solar magnetic field, it is important to implement high-latitude solar magnetic field monitoring that obtains simultaneous polar views. These would provide information available in no other way. If stationed in orbit at 1 AU, a near polar orbit could provide satisfactory cadence to follow the polar magnetic field evolution over the solar cycle, but an orbital pair would be best. The gravity-assisted high-inclination Ulysses mission [*Wenzel et al*., 1992] and the success of the Dawn solar electric propulsion system [*Russell and Raymond*, 2011] in visiting objects with differing ecliptic inclinations demonstrate that such solar polar orbits are achievable with current technologies.

As for the sunspot cycle and its predictability based solely on sunspot number behavior, the current results suggest that only modest improvements may be possible. While insight into the sunspot-dynamo relationship will likely improve in the near term, there will also likely be a sufficiently large number of variables involved that improvement on the empirical Waldmeier relationships is unlikely. Nevertheless, the long term history of solar behavior represented by the sunspot record will continue to give it a unique advantage for both retrospective studies of the Sun and for prediction (including of its extremes) in a probabilistic sense. Continuing collection of such long-term synoptic data continues to be an essential part of making further progress.

Acknowledgments

This work was supported by Predictive Science, (P. Riley) and STEREO (through a NASA grant NNX15AG09G for the IMPACT Investigation). The data used in this paper are available in the archive, Sunspot Index and Long-Term Solar Observations (SILSO) at the Royal Observatory of Belgium (http://sidc.be/silso/). LKJ's work is supported by the NASA LWS and HSR programs. JGL's work is supported by NASA grant 80NSSC18K1446 from the Heliophysics Division.

Glossary

Dawn: Discovery-class mission using ion propulsion to orbit two different main belt asteroids with different inclinations to the ecliptic plane.

Dynamo: An electric current generator. The Sun and some planets have internal dynamos that generate large-scale sometimes very strong magnetic fields that can periodically reverse.

Grand cycle: A set of solar cycles in which the onset of solar minimum becomes earlier and earlier measured on an 11.05yr clock ending with a resetting of the phase to that of the 11.05yr clock and the occurrence of a lower than normal solar maximum sunspot count.

Hadley cell: Atmospheric circulation that rises in the equatorial region and sinks at middle latitudes.

Hale's law: Sunspots generally consist at regions of both positive and negative polarity. A group of sunspots usually have one leading polarity and the opposite trailing polarity. Generally the opposite behavior is seen in the hemisphere on the opposite side of the equator.

Helioseismology: A technique that utilizes measurements of motions of material over the solar surface to infer the structures and motions inside the Sun. This technique relies on some of the same concepts as are used when earthquakes occur, sending pressure waves throughout Earth's interior and providing information on its internal layers and core. In the case of helioseismology, detectable up and down motions due to the presence of sound waves in the near-surface gas provide information on large scale motions such as rotation all the way to the Sun's core, and on smaller scale motions just below the surface. These measurements have revealed some critical clues on the likely operation of the solar dynamo, which depends on shear or relative motions of different layers, as well as less-ordered 'turbulent' or irregular motions on all scales. The techniques of helioseismology are still improving and may represent our best chance of understanding how the solar dynamo works.

Joy's law: The tendency of sunspot groups to be tilted with the leading spot closer to the equator than following spots and to be at a large angle farther from the equator.

Maunder minimum: A period when sunspots were exceedingly rare, roughly spanning 1645 to 1715. It is named after the solar astronomer Edward W. Maunder. It coincides with the middle and the coldest part of the Little Ice Age.

Photosphere: The layer of the Sun from which photons are emitted and reach the Earth.

Poloidal magnetic flux: Magnetic field in planes defined by the axis of rotation and the radial vector in the equatorial plane.

Quadrupolar magnetic field: A magnetic field formed by two separated dipoles. The separation may be along the axis of symmetry or perpendicular to it. These produce two different magnetic field configurations.

Solar activity: Occurrence of sunspots, flares, coronal mass ejections, and many other phenomena.

Solar electric propulsion: An engine that uses electric power provided by solar panels or a generator to accelerate fuel to very high speeds and getting high efficiency (momentum) from the fuel. Acceleration can be electrostatic as used on Dawn, or magnetic (Hall thrusters) as used on the Psyche mission. Hall thrusters have more thrust but lower efficiency.

Sunspot: Dark areas on the Sun's photosphere in a white-light image. In sunspots, the magnetic field is intense, so convection is inhibited and the surface temperature is cooler than in other regions.

Sunspot cycle: The interval determined by counting the frequency and determining the solar latitude of sunspots visible on the Sun. It is about 11 years on average.

Super cycle: Occasional sunspot cycles that are extremely active.

Tachocline: The transition region in the Sun between the radiative interior and the convective outer zone. This layer is about two-thirds of the way outward from the center of the Sun. The solar dynamo is thought to arise in this region.

Taylor column: A rotating column of fluid parallel to the axis of rotation of a rotating fluid. Associated with the Coriolis effect.

Toroidal magnetic flux: Magnetic field parallel to lines of constant latitude.

Torsional oscillation: The rotation of the Sun is generally determined by tracking surface features across the disk. Historical observations showed that these features do not generally take the same time at all latitudes. Instead there is a pattern suggesting faster rotation at the equator (at a period of ~ 25 days) and slower rotation at high latitudes nearer the poles (~30 days). However, the average trends of this latitude dependence are perturbed by jet-stream-like bands that move faster or slower than the average in each hemisphere. These bands are referred to as torsional oscillations. These bands seem to follow the latitudes of active region emergence, e.g. with each band drifting toward the equator with the band of sunspot activity as the cycle progresses. The origin and consequences of these torsional oscillations is still under investigation. They also appear to be present beneath the photosphere according to helioseismological measurements.

Ulysses mission: A joint mission of NASA and ESA, and also the first mission to study the unexplored region of space above the Sun's poles. It was launched in October 1990 and ended in 2008 on its third polar orbit.

Waldmeier effect: There are two Waldmeier effects. The first but less referenced effect is that the maximum sunspot number is related to the rise time of the cycle, with shorter rise times related to stronger cycles. The more frequently referred to second effect is the observed strong correlation between the rate of increase of sunspots during a solar cycle and the maximum sunspot number achieved.

References

Babcock, H.W. (1961). The topology of the Sun's magnetic field and the 22-year cycle. *Ap. J.*, *133*, 572. https://doi.10.1086/147060.

Cao, H., Yadav, R.K., & Aurnou, J.M. (2018). Geomagnetic polar minima do not arise from steady meridional circulation. *Proc. Nat. Acad. Sci.*, *115*, 44, 11186-11191. https://doi.10.1022/pnas1717454115.

Cameron, R.H., Dikpati, M., & Brandenburg, A. (2016). The global solar dynamo. *Space Sci. Rev.*, *210*, 367-395. https://doi.10.1007/s11214-015-0230-3.

Cameron, R.H., Jiang, J., Schussler, M., & Gizon, L. (2014). Physical causes of solar cycle variability. *J. Geophys. Res.*, *119*, 680-688. https://doi10.1002/2013JA019498.

Charbonneau, P. (2010). Dynamo models of the solar cycle, *Living Reviews in Solar Physics*, *7*, 3. https://doi10.12942/lrsp-2010-3.

Chatterjee, P., Nandy, D. & Choudhuri, A.R. (2004). Full sphere simulations of a circulation-dominated solar dynamo: Exploring the parity issue. *Astron. & Astrophys.*, *427*, 1019-1030. https://doi.org/10.1051/0004-6361:20041199.

Cheung, M.M., van Driel-Gesztelyi, L., Martinez Pillet, V., Thompson, M.J. (2017). The life cycle of active region magnetic fields. *Space Science Reviews.*, 210, 317-349. doi:10.1007/s11214-016-0259-y.

Choudhuri, A.R. (2006). Some recent developments in solar dynamo theory. *J. Astrophys. & Astron.*, *27*, 79-85. https://doi.org/10.1007/BF02702509.

Choudhuri, A.R. (2008). How far are we from a standard model of the solar dynamo? *Advances in Space Res*., *41*, 868-873. https://doi.org/10.1016/j.asr.2007.04.006.

Clette, F., Svalgaard, L., Vaquero, J.M., & Cliver, E. W. (2014). Revisiting the Sunspot Number. A 400-Year Perspective on the Solar Cycle. *Space Science Reviews*, *186*, 1-4, 35-103. https://doi.org/10.1007/s11214-014-0074-2.

Clette, F. & Lefèvre, L. (2016). The New Sunspot Number: assembling all corrections. *Solar Physics*, *291*, 9-10, 2629-2651. https://doi.org/10.1007/s11207-016-1014-y.

Clette, F., Lefèvre, L., Cagnotti, M., Cortesi, S., & Bulling, A. (2016a). The Revised Brussels-Locarno Sunspot Number (1981 - 2015). *Solar Physics*, *291*, https://doi.org/10.1007/s11207-016-0875-4.

Clette, F., Cliver E.W., Lefevre, L., Svalgaard, L., Vaquero, J.M., & Leibacher, J.W. (2016b). Preface to Topical Issue: Recalibration of the Sunspot Number, *Solar Phys.*, *291*, 9-10, 2479-2486. https://doi:10.1007/s11207-016-1017-8.

Dicke, R.H. (1978). Is there a chronometer hidden deep in the Sun? *Nature*, *276*, 676-680. https://doi:10.1038/276676b0.

Dikpati, M., & Gilman P.A. (2006). Simulating and predicting solar cycles using a flux-transport dynamo. *Ap. J.*, *649*, 498-514.

Dikpati, M., de Toma, G., & Gilman, P.A. (2006). Predicting the strength of solar cycle 24 using a flux-transport dynamo-based tool. *Geophys. Res. Lett.*, *33*, 502. https://doi.org/10.1029/2005GL025221.

Fuentes, O.V. (2009). Kelvin's discovery of Taylor columns. *European Journal of Mechanics*, *28*, 3, 469-472. https://doi.org/10.1016/j.euromechflu.2008.11.002.

Hale, G.E. (1908). On the Probable Existence of a Magnetic Field in Sun-Spots, *Ap. J.*, *28*, 315. https://doi.org/10.1086/141602.

Hathaway, D.H. (2015). The Solar Cycle. *Living Reviews in Solar Physics, 12*. https://doi.org/10.1007/lrsp-2015-4.
Hathaway, D.H. & Upton L.A. (2016). Predicting the amplitude and hemispheric asymmetry of solar cycle 25 with surface flux transport. *J. Geophys. Res., 121,* 10744-10753. https://doi.org/10.1002/2016JA023190.
Howard, R. & Labonte, B.J. (1980). The Sun is observed to be a torsional oscillator with a period of 11 years. *Ap. J. Lett., 239*, L33-L36. https://doi.org/10.1086/183286.
Howe, R. (2009). Solar interior rotation and its variation. *Living Reviews in Solar Physics, 6*. https://doi.org/10.12942/lrsp-2009-1.
Howe, R., Komm R., & Hill, F. (2000). Variations in solar subsurface rotation from GONG data 1995-1998, *Sol Phys., 192,* 427-435. https://doiorg./10.10231/A:1005202805104.
Karak, B.B. & Choudhuri, A.R. (2011). The Waldmeier effect and the flux transport dynamo. *MNRAS, 410*, 1503-1512. https://doi.org/10.1111/j.1365-2966.2010.17531.x
Karak, B.B. & Miesch, M. (2017). Solar cycle variability induced by tilt angle scatter in a Babcock-Leighton solar dynamo model. *Ap. J., 847*. https://doi.org/10.3847/1538-4357/aa8636.
Kitiashvili, I., & Kosovichev, A.G. (2008). Application of data assimilation method for predicting solar cycles. *Ap. J., 688*, L49-L52.
Komm, R., Howe, R., & Hill. F. (2018). Subsurface zonal and meridional flow during cycles 23 and 24. *Sol. Phys., 293*. https://doi.org/10.1007/s11207-018-1365-7.
Kosovichev, A.G., & Pipin, V.V. (2019). Dynamo wave patterns inside the Sun revealed by torsional oscillations. *Ap. J. Letters*, *871*. https://doi.org/10.3847/2041-8213/aafe82.
Kosovichev, A.G., & Zhao, J. (2016). Reconstruction of solar subsurfaces by local helioseismology. Chapter 2 in *Cartography of the Sun and Stars, Lecture notes in Physics 914*. https://doi:10.1007/978-3-319-24151-7-2, Springer.
Lehmann, I. (1936). *P`, Pub. Du Buraeu Central Seis. Inter., A14(3),* 87-115.
Leighton, R.B. (1969). A magneto-kinematic model of the solar cycle. *Ap. J., 156*, 1. https://doi.org/10.1086/149943.
Mahajan, S.S., Nandy, D., Antia, H.M., & Dwivedi, B.N. (2018). Toroidal oscillations of the Sun's rotation contribute to the Waldmeier Effect in solar cycles. *Solar and Stellar Astrophys.* arXiv:1803.007758v1.
McIntosh, S.W., Leamon, R.J., Gurman, J.B., Olive, J.-P., Cirtain, J.W., & Hathaway, D.H. et al. (2013). Hemispheric asymmetries of solar photospheric magnetism: Radiative, particulate, and heliospheric impacts. *Astrophys. J., 765*, 146. https://doiorg/10.1088/0004-637X/765/2/146.
McIntosh, S.W., Wang, X., & Leamon, R.J., Howe, R., Krista, L.D., & Malanushenk, A.V. et al. (2014), Deciphering solar magnetic activity. I. On the relationship between the sunspot cycle and the evolution of small magnetic features, *Astrophy. J*., *792*, 12. https://doi.org/10.1088/0004-637X/792/1/12.
Miesch, M.S. (2005). Large scale dynamics of the convection zone and tachocline. *Living Reviews in Solar Physics*, *2*. https://doi.org/10.12942/lrsp-2005-1.
Murakozy, J. & Ludmany, A. (2012). Phase lags of solar hemispheric cycles. *MNRAS, 419,* 3624-3630. https://doi.org/arXiv/1309.2114.
Passos, D., Nandy, D., Hazra, S., & Lopes, I. (2013). A solar dynamo model driven by mean field alpha and Babcock-Leighton sources: Fluctuations, grand minima-maxima, and hemispheric asymmetry in sunspot cycles. *Astron. & Astrophys., 563*. https://doi.org/10.1051/0004-6361/201322635.
Pesnell, W.D. & Schatten, K.H. (2018). An early prediction of the amplitude of Solar Cycle 25. *Solar Phys., 293,* 7. https://doi.org/10.1007/s11208-08-1330-5.

Pipin, V.V., & Kosovichev, A.G. (2011). The asymmetry of sunspot cycles and Waldmeier relations as a result of nonlinear surface-shear shaped dynamo. *Ap. J.*, *741*, 1.

Pipin, V.V. &Kosovichev., A.G. (2018). Does nonaxisymmetric dynamo operate in the Sun? arXiv:1808.05332v2.

Rempel, M. (2007). Origin of solar torsional oscillations. *Ap. J.*, *655*, 651-659.

Rempel, M., Schussler, M., Cameron, R.H., & Knolker, M. (2009). Penumbral structure and outflows in simulated sunspots. *Science*, *325*, 171-174. https://doi.org/10.1126/science1173798.

Russell, C.T., & Raymond, C.A. (2011). The Dawn Mission to Vesta and Ceres. *Space Sci. Rev.*, *163*, 1-4, 3-23. https://doi.org/10.1007/s11214-011-9386-2.

Russell, C.T., Luhmann, J. G., & Jian, L.K. (2010). How unprecedented a solar minimum? *Rev. Geophys.*, *48*, RG2004. https://doi.org/10.1029/2009RG000316.

Russell, C.T., Luhmann, J.G., & Strangeway, R.J. (2015). *Space Physics, An Introduction*, Chapter 5, Cambridge University Press, Cambridge, UK.

Schaeffer, N., Jault, D., Nataf, H.-C., & Fournier, A. (2017). Turbulent geodynamo simulations: A leap towards Earth's core. *Geophys. J. Inter.*, *2011*, 1-29. https://doi.org/10.1093/gji/ggx265.

Schatten, K.H., Scherrer, P.H., Svalgaard, L., & Wilcox, J.M. (1978). Using dynamo theory to predict the sunspot number during solar cycle 21. *Geophys. Res. Lett. 5*, 411-414. https://doi.org/10.1029/GL005i005p00411.

Schussler, M., & Cameron, R.H. (2018). Origin of the hemispheric asymmetry of solar activity. *Astron. & Astrophys*., *618*. https://doi.org/10.1051/0004-6361/201833532.

Sheeley, N.R. Jr. (2005). Evolution of the Sun's magnetic field: A historical review of the flux transport mechanism. *Living Reviews in Solar Physics*, *2*. https://doi.org/10.12942/lrsp-2005-5.

Svalgaard, L. (2013). Solar activity-Past, present, future. *J. Space Weather and Space Climate*, *3*. https://doi.org/10.1051/swsc/2013046.

Svalgaard, L. & Kamide, Y. (2013). Asymmetric solar polar field reversals. *Astrophys. J.*, *763*, 23, 1-6. https://doi.org/10.1088/0004-637X/763/1/23.

Taylor, G.I. (1922). The motion of a sphere in a rotating liquid. *Royal Society Publishing.* https://doi.org/10.1098/rspa.1922.0079.

Thompson, M.J., Christensen-Dalsgaard, J., Miesch, M.S., & Toomre, J. (2003). The internal rotation of the Sun. *Annu. Rev. Astron. Astrophys.*, *41*, 599-643. https://doi.org/10.1146/annurev.astro.41.011802.094848.

Thompson, M.J. (2004). Helioseismology and the Sun's interior. *Astron. Geophys.*, *45*, 4.21-4.25. https://doi.org/10.10145/j.1468-4004.2003.45421.x.

Waldmeier, M. (1935). *Astron. Mitt. Zurich*, 14, 105.

Temmer, M., J., Rybak, J., Bendik, P., Veronic, A., Vogler, F., & Otruba, W. et al. (2006). Hemispheric sunspot numbers Rn and Rs from 1945-2004: Catalogue and N-S asymmetry analysis for solar cycles 18-23. *A&A*, *447*, 735-743. https://doi.org/10.1051/0004-6361:20054060.

Ulrich, R.K. (2010). Solar meridional circulation from Doppler shifts of the Fe I line at 5250 angstrom as measured by the 150 foot solar tower telescope at the Mt. Wilson Observatory. *Astrophys. J.*, *725*, 658-669. https://doi.org/10.1088/0004-637X/725/1/658.

Wang, Y.M. (2017). Surface flux transport and the evolution of the Sun's polar fields. *Space Sci. Rev.*, *210*, 351-365. https://doi.org/10.1007/s11214-016-0257-0.

Wang, Y.M., Lean, J.L., & Sheeley, N.R. (2005). Modeling the Sun's spectral irradiance since 1713. *Astrophysical Journal*, *625*, 522-548.

Wenzel, K.P., Marsden, R.G., Page, D.E., & Smith, E.J. (1992), The Ulysses mission. *Astron. Astrophys. Suppl. Series*, *92*, 207-219.

Wilson, P.R., Altrocki, R.C., Harvey, K.L., Martin, S.F., & Snodgrass, H.B. (1988). The extended solar activity cycle. *Nature*, *333*, 748.

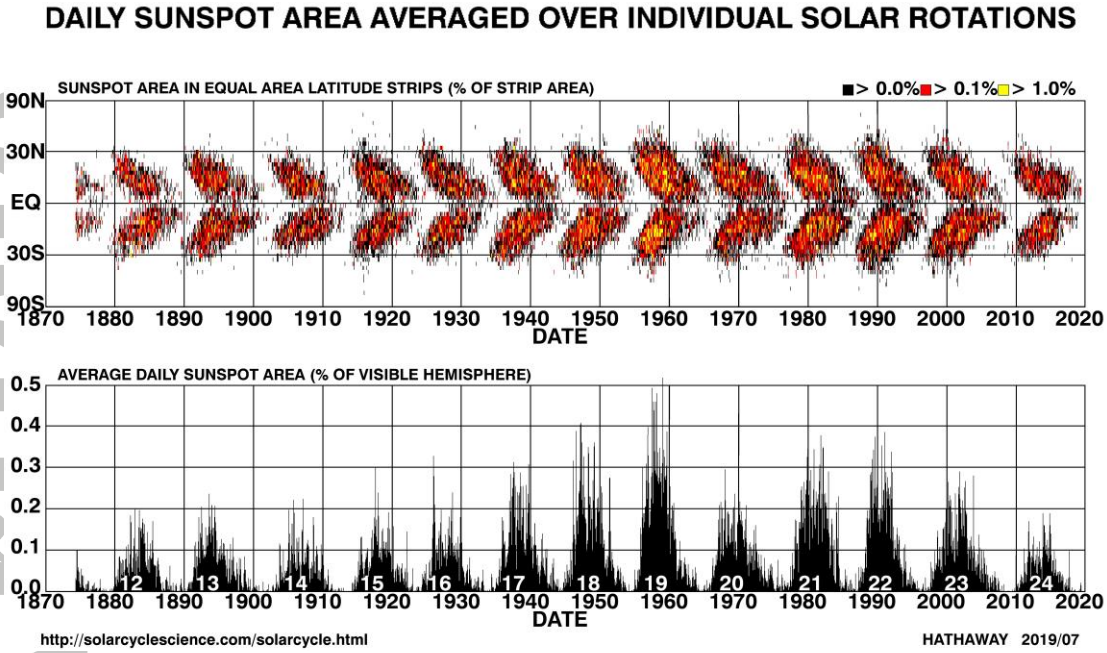

Figure 1. Plot (from SolarCycleScience.com, D. Hathaway) of the cumulative sunspot locations (latitudes) on the visible disk (top panel), known as the butterfly diagram display, and the corresponding daily sunspot areas (fractions of visible hemisphere) on the photosphere (bottom panel).

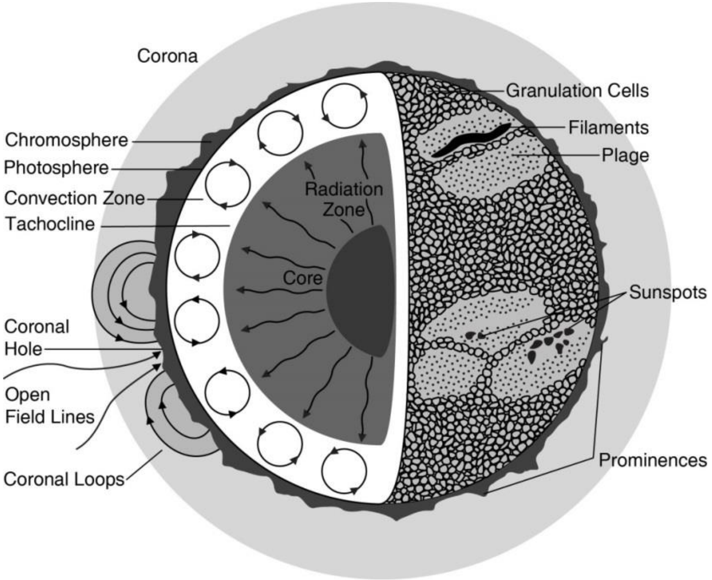

Figure 2. The structure of the Sun. The interior structure of the Sun is on the left, while the phenomena on the surface are shown on the right. Sunspots are seen equally in both hemispheres, but with opposite magnetic symmetries. Leading and trailing polarities are opposite in the two hemispheres and reverse every sunspot cycle. (Russell et al., 2015)

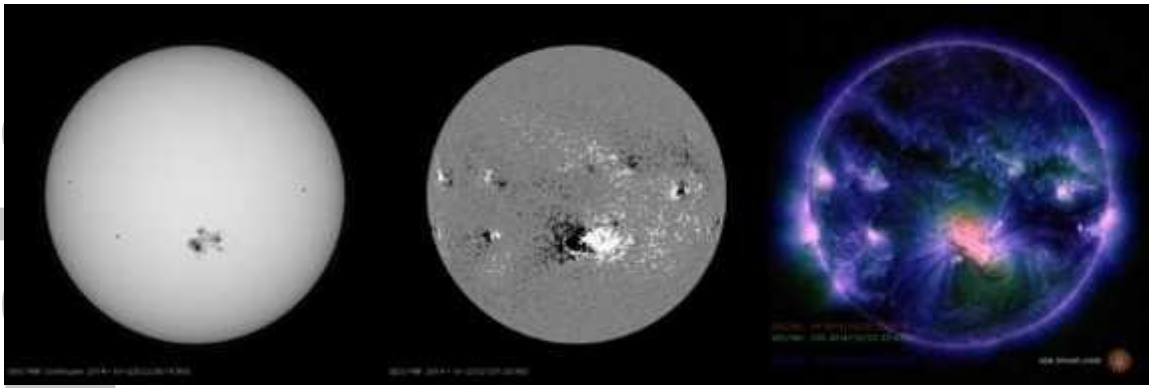

Figure 3. This figure from *Cheung et al* [2017], illustrates the relationships between (left) sunspots seen in the visible disk image, (center) the magnetic field strengths and polarities seen with a magnetograph (shown in gray scale with black and white the strongest inward and outward fields), and (right) the Extreme Ultraviolet image showing coronal loops over the strongest field regions. Note that not all magnetic features show up as sunspots. Also, the magnetic bipoles, that the stronger active regions form, are ordered with opposite leading (right-most, in the sense of rotation) field polarities depending on the hemisphere, and are tilted with the leading pole generally closer to the equator. The leading field polarities match the (barely distinguishable) polar fields in their hemisphere through the cycles rising phase and maximum.

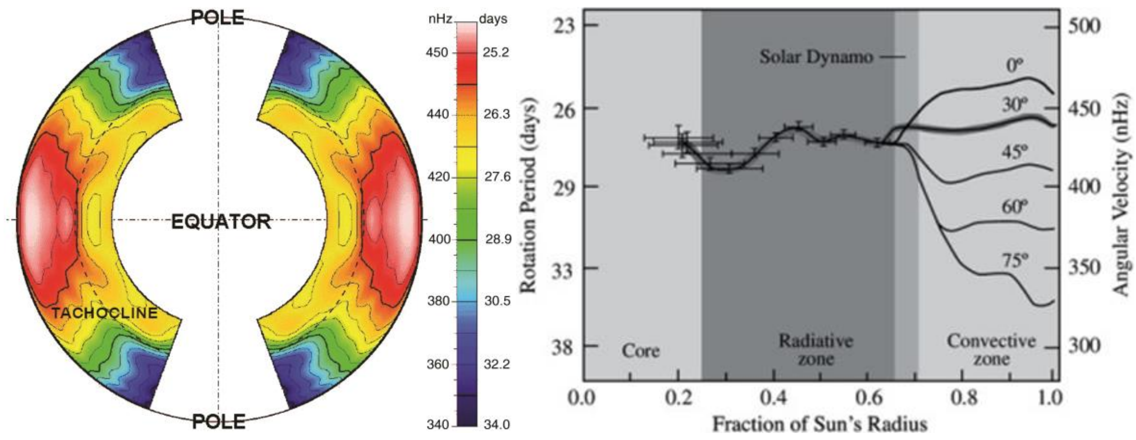

Figure 4. Internal structure of the Sun's rotation, showing the location of the tachocline where rigid rotation gives way to differential rotation throughout the convection zone (left), and the rotation period as a function of radius (right) at different latitudes. In the left panel, the color scales are for solar differential rotation frequency (nHz) and the corresponding rotation period (day). In the righthand panel the latitude where zonal velocity transitions from effective super rotation at low latitudes, to sub rotation at mid and high latitudes, occurs at around 30 degrees. The torsional oscillation (see later text) tends to initially appear around 55 degrees, while the associated surface magnetic activity appears with it after it has migrated to ~30 degrees. The reasons for this behavior have yet to be determined. (left) Figure is adapted from NASA MSFC (https://solarscience.msfc.nasa.gov/images/internal_rotation_mjt.jpg). (right) Courtesy of K.R. Lang, Tufts University (https://ase.tufts.edu/cosmos/print_images.asp?id=25). These figures are respectively adaptations of the original results from helioseismology published by Thompson et al. [2003] and the National Solar Observatory (NSO).

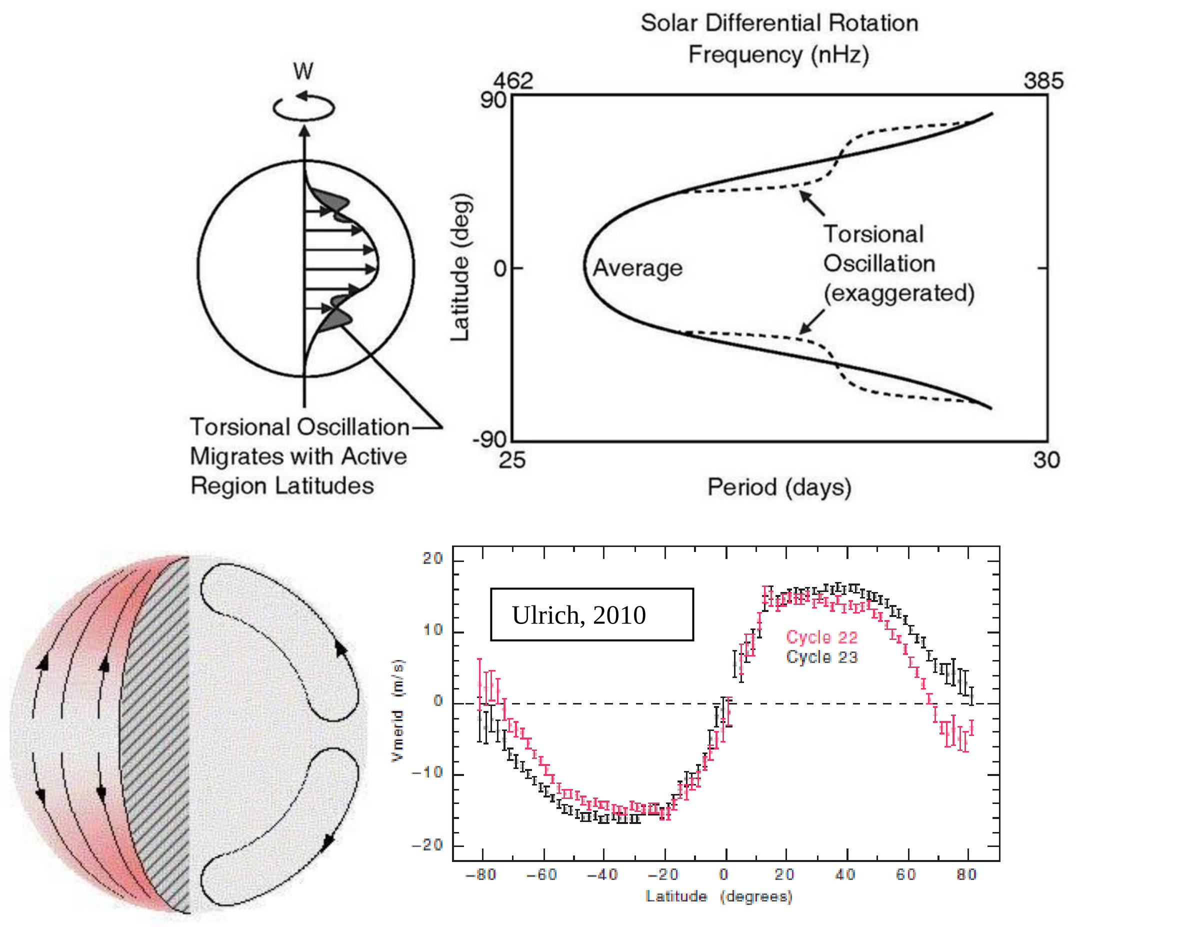

Figure 5. Illustrations of the torsional oscillations (top) and meridional circulation (bottom) described in the text.

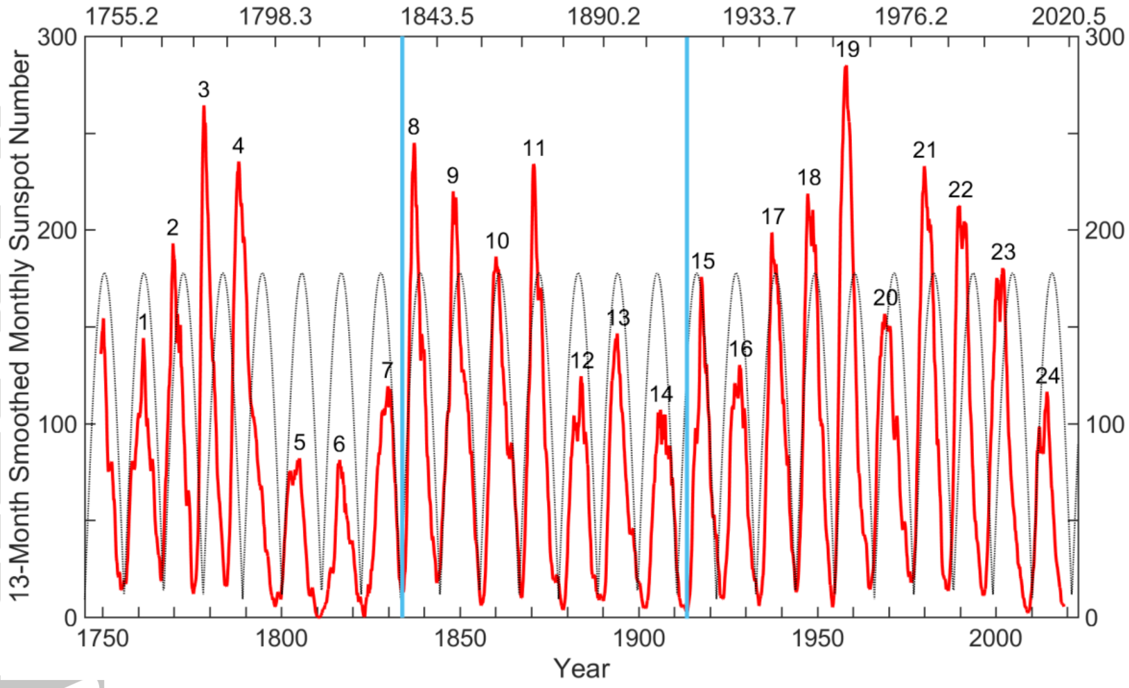

Figure 6. Sunspot record since 1749, solid red line. The dotted line is an 11.05 yr period cycle with amplitude of 178.7, the average maximum SSN of cycles 1-24, for the current sunspot maxima. The 11.05-yr period is the average period for cycles 1-23. At the top abscissa axis, the ticks mark the time of solar minima.

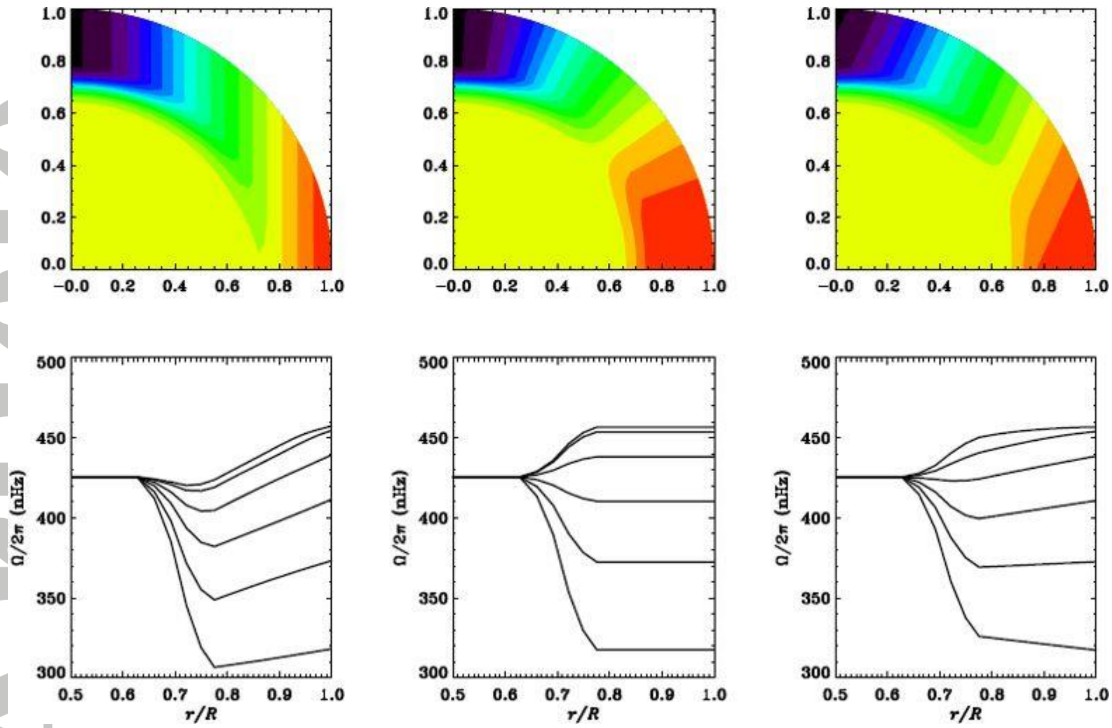

Figure 7. Modeling results of the convection zone rotational velocity contours and constant latitude radial profiles in a similar format as Figure 4 [*Howe et al.*, 2009]. Here, the left-most panel shows the rotational velocity pattern that would be associated with Taylor-Proudman columns that are characteristic of a fluid in a rotating chamber. The center panel shows rotation that depends on latitude, and the rightmost panel shows a model close to the observed pattern, which is somewhere between the other two. For dynamo models that simulate convection zone circulation, achieving the latter result would be one mark of success. Red indicates fast rotation and blue, slow.

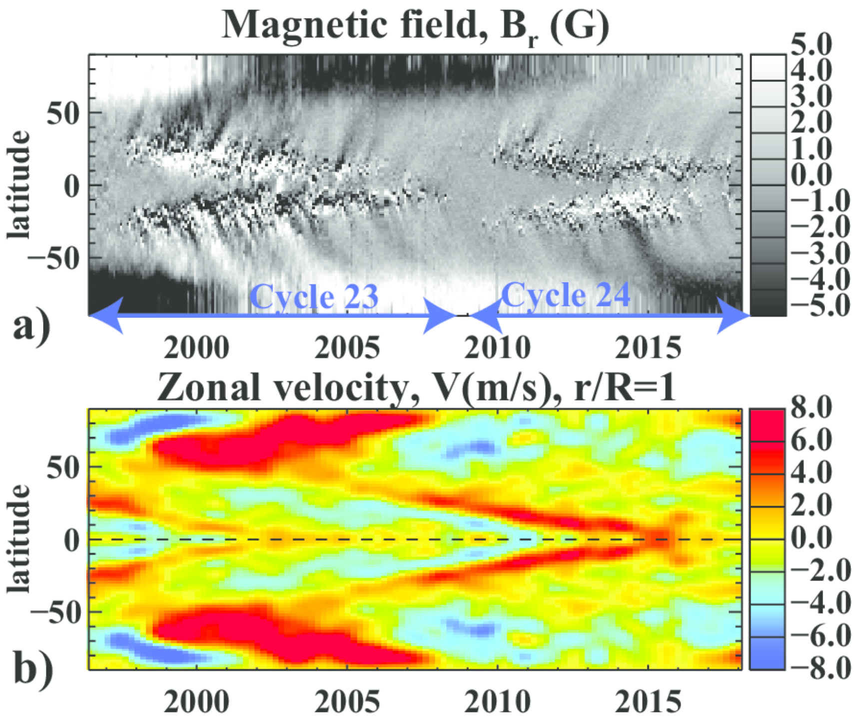

Figure 8. Figure adapted from Kosovichev and Pipin (2019), illustrating the cyclic behavior of the torsional oscillation velocity in the lower panel (b), compared with the solar magnetic cycle as seen in the longitudinally averaged radial surface magnetic field (a). The similarity of these patterns, which both showing poleward and equatorward branching features, suggests they are related (see text).

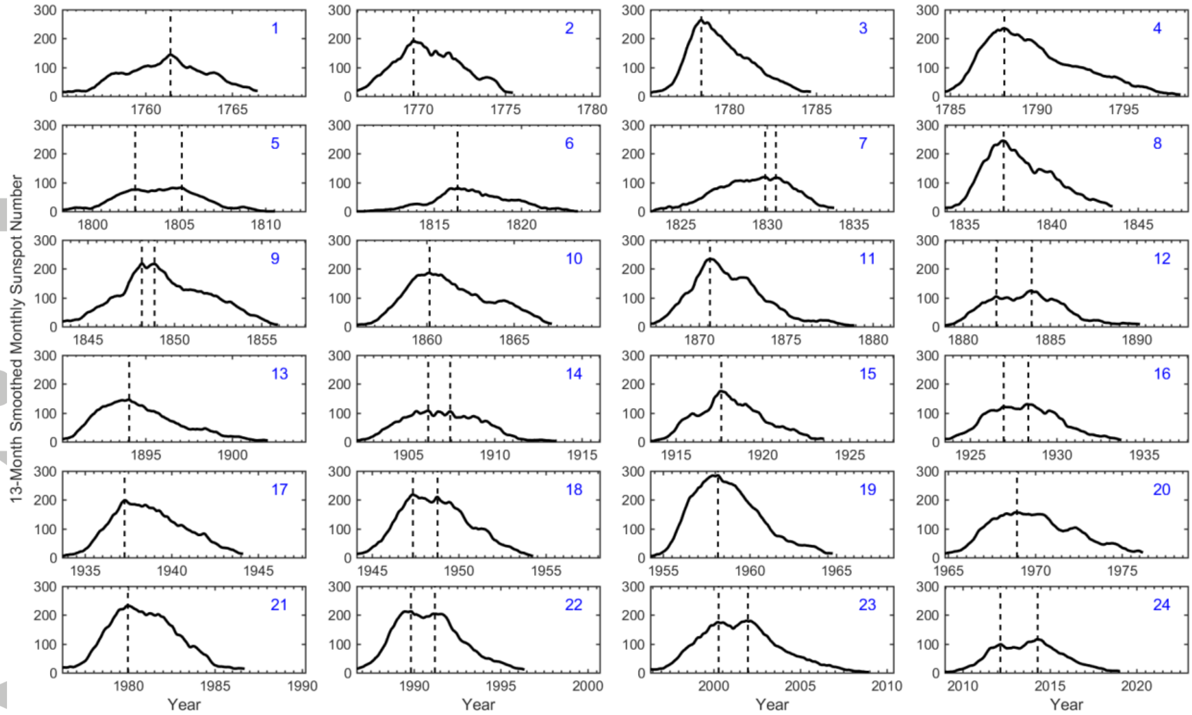

Figure 9. Sunspot number cycle shapes used in this study. The 13-month smoothed SSN from SILSO is used. Each panel presents one solar cycle with a fixed 14-year interval for the abscissa axis, and the dashed vertical line marks the SSN maximum (two peaks in some cycles).

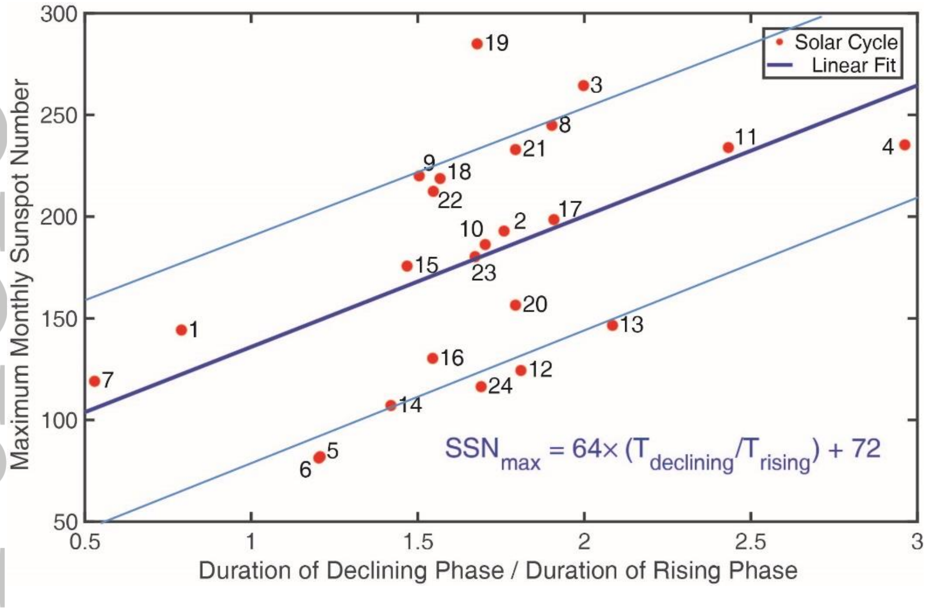

Figure 10. Maximum monthly sunspot number for cycles 1 – 24 plotted versus the duration of the declining phase divided by the duration of the rising phase ($T_{declining}/T_{rising}$). The central line is the best fit to all the points, given by the equation shown. The bracketing lines suggest limits within which the points generally fall. Mid-2020 is assumed to be the end of cycle 24.

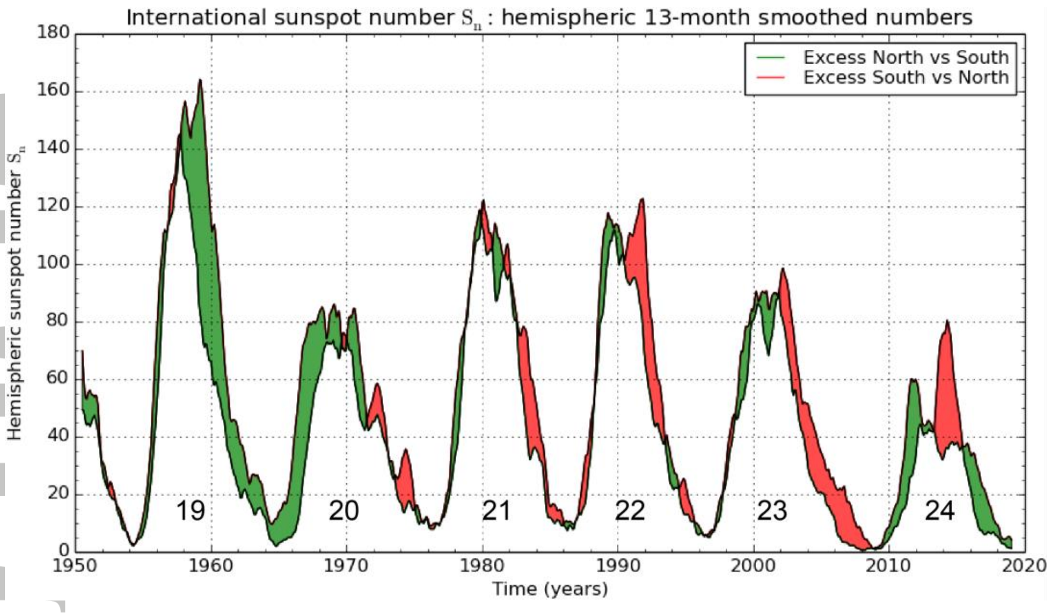

Figure 11. Plot of 13-month smoothed monthly sunspots in each hemisphere separately. Green shading indicates north excess over south. Red indicates south excess over north. Cycle numbers are marked. From SILSO at Royal Observatory of Belgium.

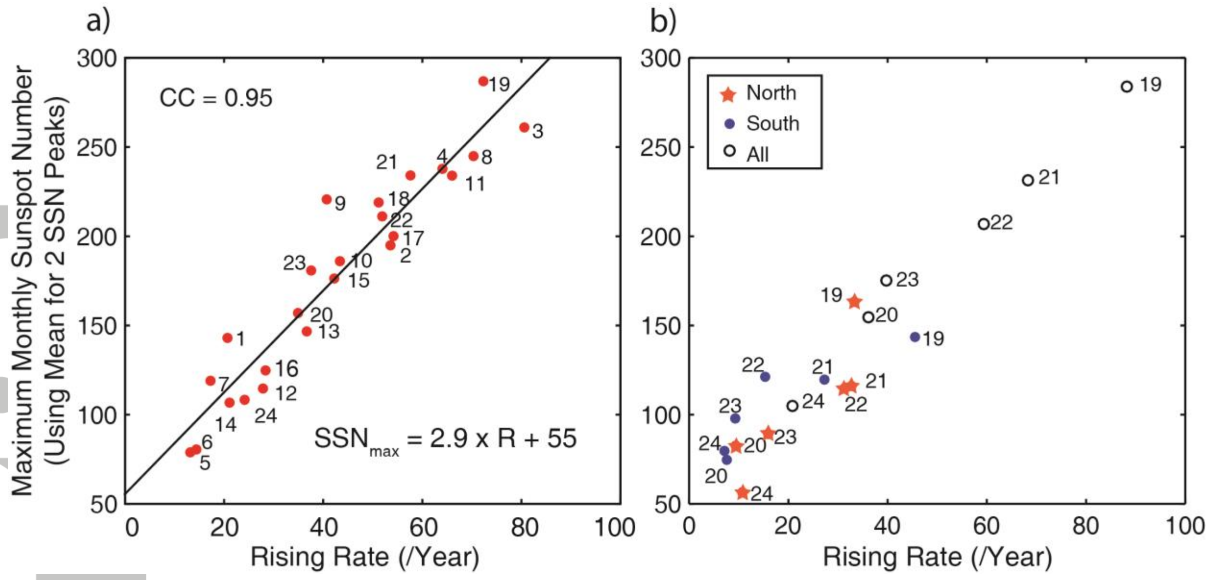

Figure 12. a) Reconstruction of the Waldmeier Effect 2 relationship showing the remarkably close relationship between the cycle maximum and the sunspot number rise rate for the full-disk SSN (left). b) The same plot for the hemispheric SSN (red for north, blue for south) shows the hemispheric differences. For comparison, the black empty circles are for all SSN as shown in a). Note the abscissa scales are different between two panels.